

Experimental characterization of droplet dispensing in electrowetting-based microfluidics

Mohammad Khorsand Ahmadi, Mehrdad Shokoohi, and Mohammad Passandideh-Fard

Citation: *Appl. Phys. Lett.* **111**, 043701 (2017); doi: 10.1063/1.4996364

View online: <http://dx.doi.org/10.1063/1.4996364>

View Table of Contents: <http://aip.scitation.org/toc/apl/111/4>

Published by the [American Institute of Physics](#)



Experimental characterization of droplet dispensing in electrowetting-based microfluidics

Mohammad Khorsand Ahmadi, Mehرداد Shokoohi, and Mohammad Passandideh-Fard^{a)}
 Department of Mechanical Engineering, Ferdowsi University of Mashhad, Mashhad, Iran

(Received 26 April 2017; accepted 16 July 2017; published online 25 July 2017)

In this study, the effect of various parameters on the dispensed droplet size in microchannels based on the electrowetting on dielectric technique is experimentally investigated. A printed circuit board (PCB)-based microfluidic chip is used as a platform for the experiments. A crescent configuration for the channel electrodes is fabricated, which leads to a higher electrowetting force which improves the motion of the droplet. In addition, two electrode designs are proposed, which provide a nearly constant overlapping length on the reservoir electrode. The focus of this paper is on the geometry of the reservoir and the channel electrode; therefore, the channel dimensions, surface conditions, and applied voltage are kept constant. The experiments are performed for various reservoir liquid volumes and different electrode shapes of the reservoir and the microchannel. The results show that decreasing the length of the small reservoir electrode reduces the size of the dispensed droplet. It is also observed that using a channel electrode curved in the opposite direction of the droplet motion leads to a smaller dispensed droplet. *Published by AIP Publishing.*

[<http://dx.doi.org/10.1063/1.4996364>]

From the early 1980s, microfluidics has been developing as an efficient tool for many research areas and more specifically for biological analysis. This new technology promises to provide the benefits of high portability and controllability, faster analysis due to shorter reactions, and low fabrication cost. Digital microfluidics (DMF) is a technique used in a wide range of applications reported in the literature such as immunoassay preparation,^{1–3} point-of-care diagnostics,^{4,5} optical microdevices,^{6,7} proteomic sample preparation, DNA ligation, and simple separations.⁸ The electrowetting on dielectric (EWOD) is the most popular method used to actuate and manipulate the microdroplets in DMF systems. It is utilized in other applications such as microswitches,⁹ electrowetting displays,¹⁰ and liquid lenses.^{11–13} Applying the EWOD technique, microdroplets can be driven towards any specific position without the need for a micro-pump and a micro-valve. In the EWOD method, the wettability of a dielectric coated metallic substrate (electrode) exposed to a liquid droplet is increased when an electric potential difference is applied between the liquid and the electrode. Lippmann¹⁴ in 1875 for the first time reported this phenomenon when he observed more wettability of mercury by applying an electric potential difference. In the equilibrium condition, when a droplet is on the solid surface, the external forces are balanced and surface energy becomes minimum. Applying an electrical field will upset the original equilibrium condition, and the droplet will change its contact angle according to the Young–Lippmann mathematical equation

$$\cos(\theta_v) = \cos(\theta_0) + \frac{\epsilon_0 \epsilon_d}{2 d \gamma_{LG}} V^2, \quad (1)$$

where θ_0 is the contact angle of the droplet in the absence of voltage V , θ_v is the droplet contact angle when applying

voltage, ϵ_d is the dielectric constant of the insulated layer, ϵ_0 is the permittivity of vacuum, d is the thickness of the insulator, and γ_{LG} refers to the surface tension of the droplet at the liquid-gas interface.

In DMF systems, individual microdroplets are dispensed, transported, merged, mixed, and split into smaller segments. In particular, the droplet dispensing is one of the most difficult manipulations to be accomplished. The size of the dispensed droplet depends on numerous factors such as the applied voltage, reservoir liquid volume, surface condition, size of the reservoir electrode, location of pinch-off, and channel dimensions.

In recent years, many studies have been conducted to investigate various parameters that can influence the droplet movement, applied voltage, reproducibility, and size of the dispensed droplet.^{15–18} An assessment of long-term reproducibility of droplet dispensing in digital microfluidic devices was done by Elvira *et al.*¹⁹ They obtained dispensing droplets from a reservoir by measuring the volume of both the droplet and the reservoir liquid and then returning the dispensed droplet to the reservoir. The repetition of this process was accomplished over the course of several hundred iterations. Their results showed that spacing between the plates influences the reliability of droplet dispensing. Wang *et al.*²⁰ introduced a certain electrode shape to improve the reproducibility of droplet dispensing. They designed an electrode with two outer arcs and a center dumbbell, imitating the natural shape of the cutting process by various widths of necking. Their results indicated that a reduction in the necking width leads to the more repeatability of the dispensed droplet.

A matter of interest in the field of microfluidics is to obtain the present size of the dispensed droplet from a reservoir by the EWOD method. Although there are multiple parameters that affect the final size of the dispensed droplet, the focus of this study is on the geometry of the reservoir

^{a)} Author to whom correspondence should be addressed: mpfard@um.ac.ir.
 Tel.: +98-51-38805022, Fax: +98-51-38807185.

electrode. In addition, as reviewed above, only a few studies performing experiments for dispensing droplets from a reservoir into a microchannel are available in the literature. Therefore, in this paper, the effects of the reservoir liquid volume, reservoir electrode length, and channel electrode shape on droplet dispensing into a microchannel are experimentally investigated. The microfluidic chip used to conduct the experiments is fabricated by employing a low cost and straightforward technique. Droplets are dispensed in air medium. Different reservoir liquid volumes as well as reservoir electrode lengths and channel electrode shapes are examined. The effect of each parameter on the dispensed droplet volume is discussed. The present work would be helpful for understanding the effects of various parameters on the dispensed droplet from a reservoir into a microchannel and could provide useful information on how to dispense droplets of uniform size.

The key physical parameters in the electrowetting on dielectric devices are the size and configuration of electrodes and channel dimensions. In order to improve the droplet motion and increase the overlapping area and electrowetting force, a crescent channel electrode configuration is employed. Compared to other electrode shapes, the crescent electrode results in a less complexity and fabrication cost. The curvature radius of the electrode is set at $1000\ \mu\text{m}$, and the space between two adjacent electrodes is set at $85\ \mu\text{m}$. The dimensions of the channel electrode shapes are shown in Fig. 1(a). For the reservoir electrode structure in Fig. 1(b), the SR and BR electrodes refer to the smaller and bigger reservoir electrodes, respectively. The purpose of the SR electrode is to keep the liquid near the entrance of the channel, while the BR electrode exerts a large force on the droplet. L_s and L_b represent the length of the SR and BR electrodes, respectively.

The printed circuit boards (PCBs) and the Fluorine Tin Oxide (FTO) glass serve as the bottom and top plates of the chip, respectively. In addition, the polyvinyl chloride (PVC) sheet forms the side walls of the microchannels. The fabrication process for the PCB which is used as the bottom plate is the customary process used to build typical printed circuit boards. A fiberglass substrate of grade FR-4 with a thickness of $1.53\ \text{mm}$ laminated by a $30\text{-}\mu\text{m}$ -thick copper layer is used as the starting material. This board is coated with a positive photoresist. A photomask carrier, containing the photomask with the electrode pattern, is placed on the photoresist and exposed to a UV beam to remove the photoresist from the areas where the copper coating should be erased. Next, the

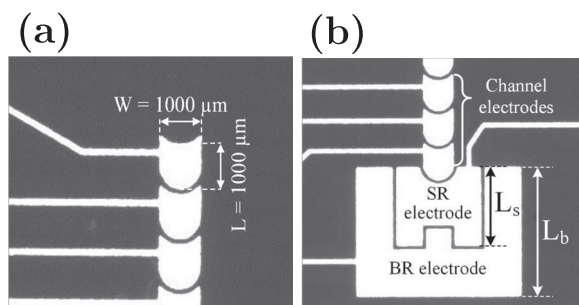


FIG. 1. (a) Dimensions of channel electrodes and (b) geometrical parameters of reservoir electrodes.

copper laminate is eliminated from the areas without photoresist coating by the acid etching technique. As a result, the pattern of electrodes takes form. An FTO coated transparent glass slide is used as the top plate of the chip. The FTO solution is sprayed on glass slides kept at $450\ ^\circ\text{C}$ for 20 min to form a $300\ \text{nm}$ FTO coating with a surface resistance of 6 Ohms per square. A commercial liquid repellent coating spray (Rust-Oleum® NeverWet®) is used as a hydrophobic layer. A dimensionless electrowetting number which is usually reported in the experiments²¹ is defined as $\eta = \frac{\epsilon_0 \epsilon_d}{2d_{TLD}} V^2$. For the entire experiments performed in this study, this dimensionless number was 0.85. A 50 Hz power supply is used to generate an AC sinusoidal wave voltage. The voltage is amplified to desired values utilizing an AC voltage amplifier. The CCD camera used in the experiments is purchased from the Grasshopper series, Point Grey Inc.

An evaluation of measurement errors is necessary to perform a reliable experiment. The experimental uncertainty due to the repeatability of the measurement (i.e., the standard uncertainty) can be calculated using the following equations:^{22,23}

$$\bar{x} = \frac{\sum_{j=1}^n x_j}{n}, \quad (2)$$

$$s = \sqrt{\frac{\sum_{i=1}^n (x_i - \bar{x})^2}{n-1}}, \quad (3)$$

$$u_{st} = \frac{s}{\sqrt{n}}, \quad (4)$$

where \bar{x} is the best estimate of x on the measured values x_1, \dots, x_n . This average is obtained from a number, n , of test results according to (2). s is the standard deviation which characterizes the average uncertainty in separate measured values x_1, \dots, x_n . The standard deviation of the mean, u_{st} , characterizes the uncertainty in the mean \bar{x} . Dividing u_{st} by the mean value results in the uncertainty due to the repeatability of measurements. The uncertainty analysis is performed for several cases, and the results are presented in Table I. For each case, the experiment is repeated three to five times. Next, the average value of the dispensed droplet volume and the corresponding uncertainty are reported. For all cases, the actuation voltage, microchannel dimensions, the size of the electrodes, and the L_s/L_b ratio are kept constant. The only variable is the reservoir liquid volume which is increased from 740 nl for case 1 to 1440 nl for case 8. The uncertainties associated with the measuring instruments are also reported in Table II.

The experimental conditions for the base case of droplet dispensing considered in this study are as follows. The length of the SR electrode (L_s) and the BR electrode (L_b) is 1.8 mm

TABLE I. The standard uncertainty due to the repeatability of experiments.

	Case 1	2	3	4	5	6	7	8
Dispensed droplet volume (nl)	217	215	200	198	197	187	150	133
Standard uncertainty	2.7%	4.9%	5%	5.8%	8.5%	3.2%	4.7%	7.8%

TABLE II. Equipment and its uncertainties.

Equipment and model	Measured parameter	Accuracy
Digital multimeter (VC9805)	Voltage	$\pm (0.8\% + 3)$ V
Electronic caliper (INSAIZE)	Microchannel Height	± 0.01 mm

and 4.1 mm, respectively [as shown in Fig. 1(b)], and the space between two adjacent electrodes is 85 μm . A microchannel with a width of 900 μm and a height of 200 μm is used. To start an experiment, first, using a sampler (Transferpette[®]), a volume of deionized (DI) water is dispensed into the reservoir. The process of droplet dispensing using a crescent channel electrode design is illustrated in Fig. 2. The SR electrode and the first channel electrode are turned on in sequence to keep the liquid in the reservoir near the entrance of the channel [Fig. 2(a)]. Next, the second channel electrode is turned on, which results in the liquid to be pulled out of the reservoir (extrusion) as seen in Fig. 2(b). Then, the BR electrode is turned on, and the SR and the first channel electrode are turned off. In this situation, having turned on the BR, the second channel electrode leads to a large force on the droplet in the opposite direction. This force causes droplet necking, which leads to the liquid pinch-off into the channel as observed in Figs. 2(c) and 2(d). For the base case explained above, the volume of liquid in the reservoir and that of the dispensed droplet are measured to be 1086 nl and 170 nl, respectively. These volumes are calculated by using the ImageJ software and a method given by Elvira¹⁹ as

$$\begin{aligned} \text{Total droplet volume} = & (\text{inner droplet area} \\ & * \text{microchannel height} \\ & + \text{volume of boundary region}), \end{aligned}$$

where the inner droplet volume represents the wetted area of the droplet on the top plate. The volume of the boundary region includes the curve of the droplet boundary profile based on the measured contact angle of DI water. The microchannel height is 200 μm in this study.

Several experiments are performed to examine the effect of various parameters on the size of the dispensed droplet into the microchannel. These parameters include: reservoir liquid volume, reservoir electrode length, and channel electrode shape. In this section, the extensive results of these experiments are provided.

The first parameter considered is the effect of the reservoir liquid volume. While other parameters including actuation

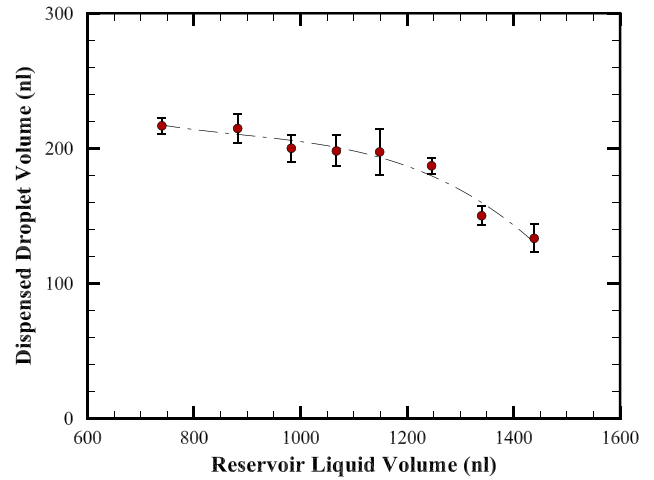


FIG. 3. The volume of the dispensed droplet versus reservoir liquid volume. All parameters are kept constant except the reservoir liquid volume. The lines are guides to the eye.

voltage, microchannel dimensions, and electrode size are kept constant, the reservoir liquid volume is increased from 740 nl to 1440 nl. A separate experiment is performed for each reservoir liquid volume by refilling the reservoir. The results of this investigation are displayed in Fig. 3 which shows how the dispensed volume varies as a function of the reservoir liquid volume. As observed explicitly in Fig. 3, the volume of the dispensed droplet is reduced by increasing the reservoir liquid volume. This result can be the consequence of several factors. The important factor is the pull-back force by the BR electrode on the droplet, which is correlated with the length of the contact line on the BR electrode. A larger overlapping area allows a significantly larger electrowetting force, which results in a smaller volume of the dispensed droplet. To further clarify this point, the force acting on the liquid can be calculated using a relation given by Wang *et al.*²⁰ as

$$F = \frac{1}{2} C_d V_d^2 L_{\text{eff}}, \quad (5)$$

where C_d is the capacitance of the dielectric layer, V_d is the applied voltage, and L_{eff} is the length of liquid contact line on the BR electrode. As observed in Fig. 3, increasing the reservoir liquid volume from 740 nl to 1150 nl (an increase of nearly 55%) results in a slight reduction in the dispensed droplet volume from 217 nl to 197 nl (a decrease of less than 9%). The small variation in the dispensed droplet volume is related to the special design of the boundary between the SR

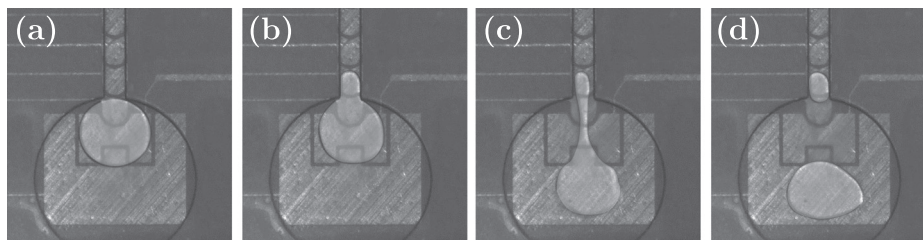


FIG. 2. The captured images of the droplet dispensing sequence using a crescent channel electrode design. To pull the liquid out from the reservoir, the channel electrodes are turned on in sequence (a) to (b). Then, both the BR electrode and the second electrode in the channel are turned on, which results in a narrow liquid necking as seen in sequence (c). The final dispensed droplet is observed in sequence (d).

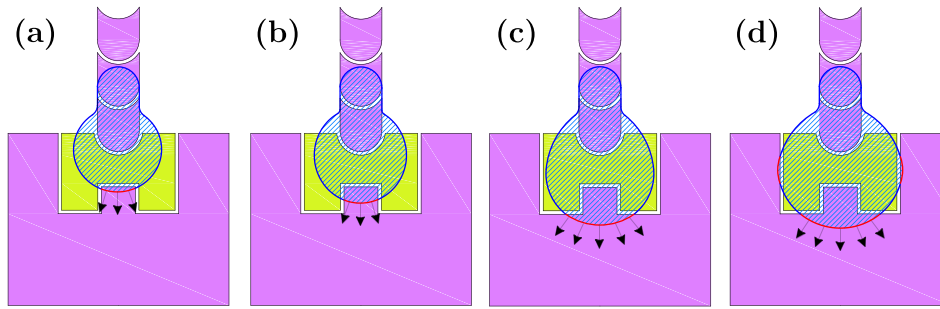


FIG. 4. A schematic of various locations of the droplet with respect to the position of the rectangular notch: (a) and (b) the contact line is inside the notch on the BR electrode, and (c) and (d) the contact line extends further from the notch.

and BR electrodes. A small rectangular notch in the boundary results in a nearly constant L_{eff} on the BR electrode while increasing the reservoir liquid volume up to a certain limit. A further increase in the reservoir liquid volume (from 1250 nl up to 1440 nl, an increase of 15%) results in the contact line to extend further from the rectangular notch causing a sudden increase in L_{eff} , which in turn leads to a faster non-linear reduction in the dispensed droplet volume (from 187 nl to 133 nl, a decrease of 29%).

Using the above special design electrode shape (with a small rectangular notch in the boundary), the dispensed droplet volume is nearly constant for different reservoir liquid volumes; therefore, this shape may be proposed for microdispensers in order to generate uniform size droplets at various remaining liquid volumes of the reservoir.

The area of the small and big reservoir electrodes covered with the liquid may be shown with A_{SR} and A_{BR} , respectively. An important parameter that affects the size of the dispensed droplet is the fraction of A_{SR}/A_{BR} . For three different cases listed in Table I, the A_{SR}/A_{BR} fraction is obtained. For case 1, the value is obtained to be $A_{SR}/A_{BR} \approx 12$. Similarly, for case 5, the fraction is $A_{SR}/A_{BR} \approx 3.8$, and for case 8, $A_{SR}/A_{BR} \approx 1.8$. As observed, decreasing the fraction of A_{SR}/A_{BR} leads to a smaller dispensed droplet. A schematic of various locations of the droplet with respect to the position of the rectangular notch is displayed in Fig. 4.

The length of the SR electrode [L_s , shown in Fig. 1(b)] is varied in several experiments, while other parameters are kept constant. The design of these electrode lengths is illustrated in Figs. 5(a)–5(c). It should be mentioned that the BR electrode length [L_b , shown in Fig. 1(b)] and shape remained constant. Figure 5(d) shows how the size of the dispensed droplet varies with the SR electrode length. This figure compares the sensitivity of the three different SR electrode lengths to the reservoir liquid volume. The ratio of the SR electrode length to that of the BR electrode is $L_s/L_b = 0.36$ in Fig. 5(a), 0.44 in Fig. 5(b), and 0.61 in Fig. 5(c). As shown in Fig. 5(d), decreasing the SR electrode length, while keeping the BR electrode length constant, results in a smaller dispensed droplet size. This can be explained by the fact that decreasing L_s would result in a shorter necking distance, which in turn makes the liquid retraction force larger and the dispensing speed faster. As a consequence, a smaller liquid volume is dispensed.

Finally, a comparison of the dispensed droplet size on experimental chips using two types of channel electrodes is made. The applied voltage, electrode dimensions, and microchannel size are kept constant. The experiments are performed for different reservoir liquid volumes. As seen in Fig. 6, two

designs for the curvature of the channel electrode shape are fabricated. Figures 6(a) and 6(b) illustrate the reverse crescent and direct crescent channel electrode designs, respectively. Figure 6(c) shows the comparison of the dispensed droplet volume measured for these two designs. As observed from the figure, for a direct crescent electrode shape in the channel, a larger droplet is dispensed. This outcome may be explained as follows: for the direct crescent shape, the liquid covers a larger portion of the channel electrode. Therefore, the overlapping length (L_{eff}) on the second channel electrode is larger, which in turn leads to a larger force on the droplet that pulls it out from the reservoir.

In this paper, the effect of various parameters on the size of a dispensed droplet from the liquid of a reservoir using the EWOD technique was experimentally examined. The parameters considered include the reservoir liquid volume, reservoir electrode length, and channel electrode shape. The actuation voltage and microchannel dimensions were kept constant. An uncertainty analysis was also performed, which showed that the uncertainty for most experiments was less than 5%. Keeping the electrode size fixed and increasing the

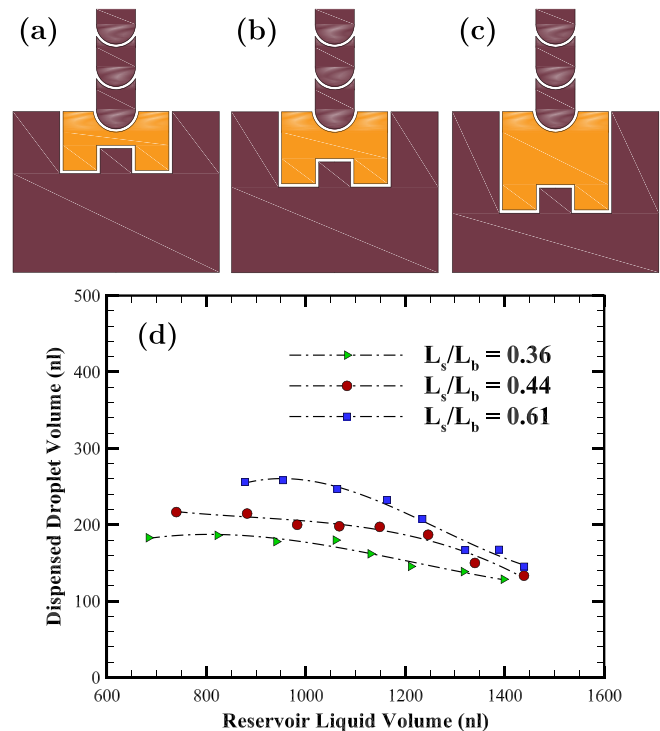


FIG. 5. (a)–(c) The top view of the schematic diagram of three different SR electrode lengths (L_s). (d) Comparison of the dispensed droplet volume using reservoir electrodes of different lengths. The lines are guides to the eye.

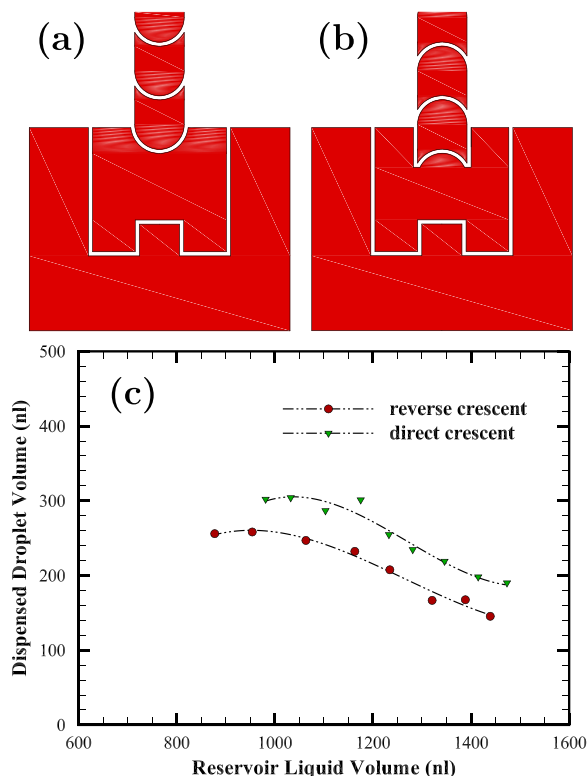


FIG. 6. The top view of the schematic diagram of (a) reverse and (b) direct crescent channel electrodes. (c) The volume of the dispensed droplet using various reservoir liquid volumes for the two channel electrode shapes of (a) and (b). The lines are guides to the eye.

reservoir liquid volume increased the length of the contact line, which in turn reduced the dispensed droplet size. It was observed that a special design of the boundary between reservoir electrodes (rectangular notch) led to a nearly uniform size of the dispensed droplet. Another investigated parameter was the length of the SR electrode [L_s , shown in Fig. 1(b)]. Decreasing this length while keeping other parameters constant led to a smaller size of the dispensed droplet. Finally, the effect of the channel electrode shape on the dispensed droplet size was studied. It was revealed that compared to the direct crescent electrode shape, the reverse crescent can

decrease the size of the dispensed droplet. Therefore, from extensive experiments performed in this study, the reverse crescent shape for the channel electrode is proposed for generating smaller dispensed droplets. The rectangular notch design for the reservoir electrode is also proposed for generating dispensed droplets of uniform size.

- ¹M. H. Shamsi, K. Choi, A. H. Ng, and A. R. Wheeler, *Lab Chip* **14**(3), 547 (2014).
- ²A. H. Ng, M. Lee, K. Choi, A. T. Fischer, J. M. Robinson, and A. R. Wheeler, *Clin. Chem.* **61**(2), 420 (2015).
- ³B. Seale, C. Lam, D. G. Rackus, M. D. Chamberlain, C. Liu, and A. R. Wheeler, *Anal. Chem.* **88**(20), 10223 (2016).
- ⁴N. A. Mousa, M. J. Jebraill, H. Yang, M. Abdelgawad, P. Metalnikov, J. Chen, A. R. Wheeler, and R. F. Casper, *Sci. Transl. Med.* **1**(1), 1ra2 (2009).
- ⁵C. Dixon, A. H. Ng, R. Fobel, M. B. Miltenburg, and A. R. Wheeler, *Lab Chip* **16**(23), 4560 (2016).
- ⁶S.-L. Lee and C.-F. Yang, *Opt. Express* **16**(24), 19995 (2008).
- ⁷H. Zeng, A. D. Feinerman, Z. Wan, and P. R. Patel, *J. Microelectromech. Syst.* **14**(2), 285 (2005).
- ⁸Y.-Y. Lin, E. R. Welch, and R. B. Fair, *Sens. Actuators, B* **173**, 338 (2012).
- ⁹P. Sen and K. Chang-Jin, *J. Microelectromech. Syst.* **18**(1), 174 (2009).
- ¹⁰H. You and A. Steckl, *Appl. Phys. Lett.* **97**(2), 023514 (2010).
- ¹¹B. Berge, in *Proceedings of the 18th IEEE International Conference on Micro Electro Mechanical Systems, MEMS*, Miami, Florida, USA (2005), p. 227.
- ¹²O. D. Supekar, M. Zohrabi, J. T. Gopinath, and V. M. Bright, *Langmuir* **33**(19), 4863 (2017).
- ¹³A. Shahini, J. Xia, Z. Zhou, Y. Zhao, and M. M.-C. Cheng, *Langmuir* **32**(6), 1658 (2016).
- ¹⁴G. Lippmann, *Ann. Chim. Phys.* **5**, 494 (1875).
- ¹⁵E. Samiei, M. Tabrizian, and M. Hoorfar, *Lab Chip* **16**(13), 2376 (2016).
- ¹⁶X. Xu, L. Sun, L. Chen, Z. Zhou, J. Xiao, and Y. Zhang, *Biomicrofluidics* **8**(6), 064107 (2014).
- ¹⁷N. Rajabi and A. Dolatabadi, *Colloids Surf., A* **365**(1), 230 (2010).
- ¹⁸S. K. Cho, H. Moon, and C.-J. Kim, *J. Microelectromech. Syst.* **12**(1), 70 (2003).
- ¹⁹K. S. Elvira, R. Leatherbarrow, J. Edel, and A. deMello, *Biomicrofluidics* **6**(2), 022003 (2012).
- ²⁰W. Wang, J. Chen, and J. Zhou, *Appl. Phys. Lett.* **108**(24), 243701 (2016).
- ²¹F. Li and F. Mugele, *Appl. Phys. Lett.* **92**(24), 244108 (2008).
- ²²J. Taylor, *Introduction to Error Analysis, the Study of Uncertainties in Physical Measurements*, 2nd ed. (University Science Books, Sausalito, CA, 1997).
- ²³M. Sardarabadi, M. Passandideh-Fard, and S. Z. Heris, *Energy* **66**, 264 (2014).